The Carboxy-Terminal Domain of Heat-Shock Factor 1 Is Largely Unfolded but Can Be Induced To Collapse into a Compact, Partially Structured State†

Narinporn Pattaramanon,‡,§ Navneet Sangha,‡,|| and Ari Gafni*,§,||,⊥

Biophysics Research Division, University of Michigan, Ann Arbor, Michigan 48109-1055, Department of Biological Chemistry, University of Michigan Medical School, Ann Arbor, Michigan 48109-0606, and Institute of Gerontology, University of Michigan, Ann Arbor, Michigan 48109-2007

Received June 6, 2006; Revised Manuscript Received November 7, 2006

ABSTRACT: Heat-shock transcription factor 1 (HSF1) is a key regulator of the expression of heat-shock proteins during the heat-shock response. The C terminus of HSF1 (CT) contains both the regulatory and transcriptional activation domains. Predictors of natural disordered regions analysis predicts and our study demonstrates that CT is predominantly natively unfolded under physiological conditions but can be induced to fold into a number of structured states under different conditions. Under physiological conditions, CT exhibits a very low abundance of secondary and tertiary structures as observed by circular dichroism, no hydrophobic core as monitored by the 6-*p*-toluidino-2-naphthalenesulfonic acid (TNS)-binding assay, a large hydrodynamic radius as measured by size-exclusion chromatography−high-performance liquid chromatography, and high structural flexibility as probed by limited proteolysis. However, secondary-structure content significantly increases at high temperatures, in acidic pH, or in the presence of trimethylamine *N*-oxide, trifluoroethanol, or a cationic surfactant. Interestingly, the hydrophobicity of "folded" CT, as monitored by the TNS-binding assay, is enhanced by acidic pH and a cationic surfactant but not by trifluoroethanol. CT also displays different patterns in the proteolytic cleavage in acidic pH and in the presence of a cationic surfactant compared with that under native condition, suggesting that CT undergoes distinct structural rearrangements.

Organisms varying from archeabacteria to eukaryotes respond to cell-threatening conditions, such as elevated temperature and chemical, physiological, or pathological stress, by rapid expression of a group of conserved proteins that help prevent unfolding or aggregation of proteins in the cell. This highly regulated response integrates stress signals with the transcriptional regulation, resulting in downstream products called heat-shock proteins (*1*−*4*).

Heat-shock transcription factor 1 (HSF1)[1] is a central regulator for the expression of heat-shock proteins during the heat-shock response (*5*). It is organized into four highly conserved functional domains. The N terminus contains a helix−turn−helix DNA-binding domain, followed by a trimerization domain, made up of a stretch of hydrophobic heptad repeat. The C terminus contains the regulatory and transcriptional activation domains (*6*−*8*). Under normal conditions, HSF1 is in an inactive monomeric state stabilized via intramolecular coiled-coil interactions between the trimerization domain at the N terminus and the hydrophobic heptad at the C terminus. When cells are under stress, HSF1 trimerizes because this intramolecular interaction is replaced by an intermolecular coiled-coil interaction between the trimerization domains of individual HSF1 monomers. It is believed that trimerization not only allows HSF1 to bind to the heat-shock elements at the promoter region but also permits an exposure of the regions responsible for the transcriptional activity of HSF1 (*9*). These accessible segments further interact with general transcription factors to allow the paused transcription machinery to be released and the transcription to proceed (*10*−*12*).

HSF1 both in its inactive and active conformations interacts with a large number of individual biological partners (*13*−*18*) . This is not surprising because the activation/deactivation pathway of HSF1 is a multistep process that is tightly regulated to ensure proper protein folding, essential for cell survival under deleterious conditions. To be able to sequentially interact with numerous partners in a considerably short time, HSF1 must either be a very large protein containing many domains or must possess a flexible structure that can easily adopt different conformations for association with different partners. HSF1 is a medium-sized transcription factor with a molecular weight of 51 kDa and has only four

† This work was supported by a grant from the Ellison Medical Foundation.

* To whom correspondence should be addressed: Biophysics Research Division, University of Michigan, 4028 Chemistry Building, 930 North University Avenue, Ann Arbor, MI 48109-1055. Telephone: (734) 615-1964. Fax: (734) 764-3323. E-mail: arigafni@umich.edu.

‡ These authors contributed equally to this work.

§ Department of Biological Chemistry, University of Michigan Medical School.

|| Biophysics Research Division, University of Michigan.

⊥ Institute of Gerontology, University of Michigan.

[1] Abbreviations: HSF1, heat-shock transcription factor 1; CT, carboxy terminus of HSF1; GST, glutathione-*S*-transferase; TN buffer, 10 mM Tris-Cl buffer at pH 7 and 10 mM NaCl; SN buffer, 10 mM sodium acetate buffer and 10 mM NaCl; SEC, size-exclusion chromatography; PONDR, predictors of natural disordered regions; TFE, trifluoroethanol; DTA, dodecyltrimethyl ammonium chloride; TMAO, trimethylamine *N*-oxide; TNS, 2-*p*-toluidinyl-6-naphthalene sulfonate; CD, circular dichroism.

10.1021/bi061124c CCC: $37.00
Published on Web 02/27/2007

functional domains. It is therefore plausible that HSF1 contains flexible or extended regions to serve as docking sites for its various partners.

Proteins with structural flexibility that allows them to interact with a variety of partners often lack a well-defined structure. In the past decade, evidence of such intrinsically unstructured proteins has been accumulating (*19*−*23*). Indeed, it is now estimated that 30% of eukaryotic proteins may be completely or partially disordered (*24*). Proteins in this group possess a nonrigid structure under physiological conditions; i.e., the molecule is extended, highly flexible, and has little secondary or tertiary structure. There are several hypotheses attempting to explain the prevalence of disordered proteins in the eukaryotic genome. (i) The flexible structural characteristics of these proteins are advantageous for the regulation of and interaction with diverse biological partners (*23*, *25*). (ii) The large intermolecular interfaces of natively disordered proteins help alleviate molecular crowding. Thus, having disordered proteins allows the cell to reduce the required population of protein by 15−30% to produce the same amount of intermolecular interfaces (*26*, *27*). (iii) The limited structure of disordered proteins may be crucial by acting as preformed structures required in interacting with their structured partners (*28*, *29*).

Playing a critical role in the heat-shock response through interacting with its biological partners and by becoming post-translationally modified, the HSF1 structure and its conformational changes during the stress response have been extensively investigated (*5*, *30*−*32*). The structures of both its DNA-binding domain and its trimerization domain (*33*, *34*) have been well-characterized; however, attempts to analyze the structure of the full-length monomeric form of HSF1 were not successful, primarily because of the difficulty in retaining the protein in its monomeric form when expressed in bacterial cells. Studies have shown that the expression of *Drosophila* or mammalian HSF-1 in *Escherichia coli* generates constitutive trimeric or higher-ordered oligomeric forms, which might be due to the lack of negative regulators in the prokaryotic system (*35*−*38*). Cloning a truncated form of HSF1 that lacks the trimerization domain might help prevent this oligomerization and allow us to investigate the structure of its least characterized carboxy-terminal domain. In this work, we analyze the structure of the carboxy-terminal half of mouse HSF1 (CT, residues 213−503) and identify factors that can contribute to the conformational changes. Our results show that CT is natively largely unfolded but can be induced to acquire secondary structure and even to collapse into a compact structure with hydrophobic clusters under certain conditions. The structural changes in CT affect its resistance to tryptic digestion and cause it to migrate slower than under physiological conditions in size-exclusion chromatography (SEC).

MATERIALS AND METHODS

Materials. Trifluoroethanol (TFE), dodecyltrimethyl ammonium chloride (DTA), trimethylamine *N*-oxide (TMAO), and 2-*p*-toluidinyl-6-naphthalene sulfonate (TNS) were purchased from Sigma-Aldrich (St. Louis, MO). Glutathione Sepharose 4 Fast Flow and PreScission Protease were purchased from Amersham Biosciences (Piscataway, NJ).

DNA Construct. The full-length plasmid cDNA of mouse HSF1 (503 amino acids) was kindly provided by Dennis Thiele (Duke University, Durham, NC). The plasmid encoding the CT (amino acid residues 212−503) was generated by the polymerase chain reaction (PCR) from the full-length HSF1 gene using the 5′ oligonucleotide primer GCGCGAATT**C**TTGAGTGACAGCAACT and the 3′ oligonucleotide primer TAGCCTCGAGTTAGGAGACAGTGGGGTCCTT. The cDNA product obtained by PCR was cloned into the *Eco*R I−*Xho* I sites of the expression vector pGEX6P-1 (Amersham Bioscience) encoding the fusion protein glutathione-*S*-transferase (GST). The final gene product has a Precission Protease cleavage site (Gly-Pro-Leu-Gly-Ser-Pro-Glu-Phe) at the amino terminus of CT, after the GST sequence. The DNA construct was verified by DNA-encoded sequencing.

Expression and Purification. GST−CT was expressed in *E. coli* strain BL21(DE3) and purified on Glutathione Sepharose 4B beads as described previously for full-length HSF1 (*39*). After GST cleavage with Precission Protease, purified CT was dialyzed overnight in 2 L of 10 mM Tris-Cl at pH 7.4 and 10 mM NaCl (TN buffer) and was concentrated using a YM-30 Centricon centrifugal filter device (Millipore, Billerica, MA). The protein concentration was measured by the Bradford method using the Bio-Rad protein assay dye reagent (BioRad, Hercules, CA). CT was more than 90% pure when analyzed by sodium dodecyl sulfate−polyacrylamide gel electrophoresis (SDS−PAGE).

Prediction of HSF1 Disorder by Predictors of Natural Disordered Regions (PONDR). Predictions of disorder in full-length HSF1 and CT were performed using PONDR (http://www.pondr.com) using the default predictor VL-XT (*40*−*42*). This predictor integrates the three neural networks: the VL1 predictor and N- and C-terminal predictors, which were trained using the disordered regions identified from missing electron density in X-ray crystallography and nuclear magnetic resonance (NMR) studies. Access to PONDR is provided by Molecular Kinetics (Indianapolis, IN; www.molecularkinetics.com; main@molecularkinetics.com)

Circular Dichroism (CD) Spectroscopy. CD spectra were recorded using a J-715 spectropolarimeter equipped with a temperature control unit (Jasco, Inc., Easton, MD) at 22 °C in 0.01 or 0.1 cm fused silica cuvettes for far- or near-UV CD, respectively. The spectra were collected (an average of 20 scans) in a spectral range of 190−260 nm (far-UV) or 260−320 nm (near-UV) with a 2 nm bandwidth, 1 s response time, and 50 nm/min scan speed. The CT concentration was 10 μM for far-UV CD and 3 μM for near-UV CD, and the protein was dissolved in TN buffer, 10 mM sodium acetate buffer and 10 mM NaCl (SN buffer), TN buffer with 1 mM DTA, TN buffer with 1 M TMAO, or TN buffer with 30% TFE. All spectra were corrected by subtracting the solvent baseline spectrum. Molar ellipticity, $[\theta]_{MR}$, was calculated (*43*), and the spectra were plotted with Kaleidagraph (Synergy Software, Reading, PA). The secondary-structure composition was estimated by CDPro developed by Sreerama et al. (*44*). The CONTINLL algorithm was applied using the IBasis value = 4 and reference set SP43.

For the CT denaturation study, guanidine−hydrochloride (Gdn-HCl) was added to final concentrations of 0.5−4 M after incubation of CT at pH 4 or in the presence of 1 mM DTA for 1 h at room temperature. Three experiments were performed under each condition. For temperature dependence studies, the spectropolarimeter was operated in the temper-

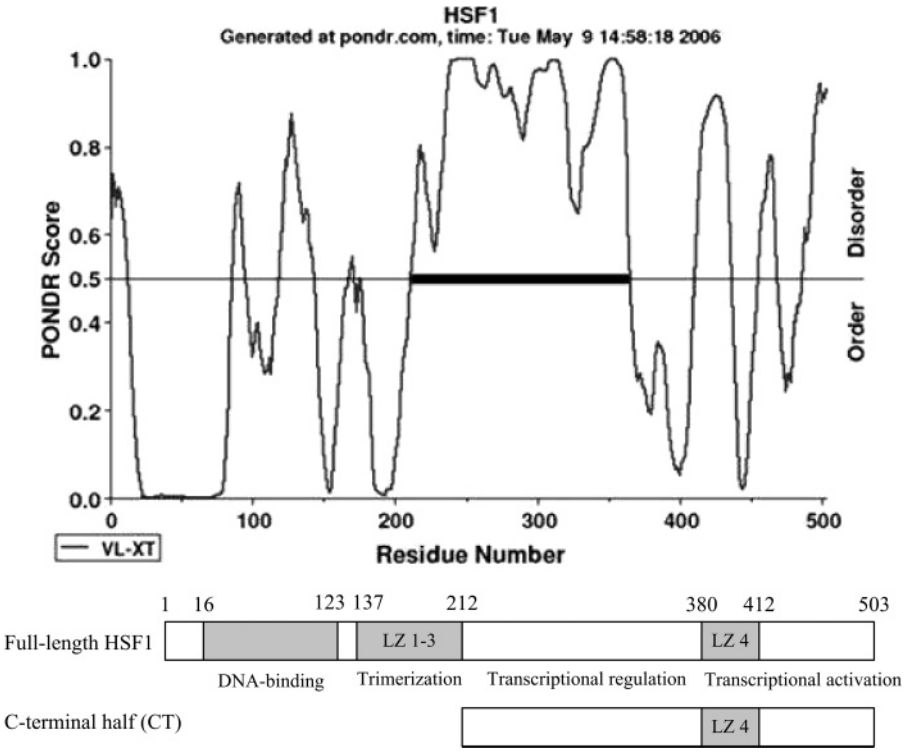

FIGURE 1: PONDR analysis of HSF1 amino acid sequences and its corresponding functional domains. The ordinate shows the predictor output values (normalized from 0 to 1), and the abscissa shows the amino acid residue number. A PONDR score output > 0.5 predicts the segment to be disordered, while a score output < 0.5 predicts the segment to be ordered. The linear diagram of the functional domains of HSF1 and CT are shown. The full-length HSF1 consists of DNA-binding, trimerization, transcriptional regulation, and transcriptional activation domains. CT contains the transcriptional regulation and activation domains. The LZ1−LZ3 (leuzine zippers 1−3) contain three hydrophobic heptads responsible for HSF1 trimerization. The LZ4 (leuzine zipper 4) is the heptad involved in the intramolecular interaction of monomeric HSF1.

ature-scanning mode and measurements were taken at λ = 222 nm through a temperature range of 20−80 °C, with an incremental rate of 1 °C/min.

Fluorescence Measurement. Fluorescence measurements were performed at 22 °C with a FP-6500 spectrofluoremeter (Jasco, Inc., Easton, MD). CT (2 μM) was incubated under different conditions for 1 h at 22 °C. Intrinsic fluorescence spectra were taken between 290 and 350 nm, with excitation at 274 nm; the excitation and emission bandwidths were 5 nm. Buffer contributions were subtracted from the raw fluorescence data to give corrected spectra.

TNS-Binding Assays. The induction of hydrophobic clusters in CT was measured with the hydrophobic probe TNS. CT (2 μM) was incubated in the desired buffer at 22 °C for 1 h. TNS (20 μM) was added, and TNS fluorescence (λ_{ex} = 310 nm, and λ_{em} = 370−500 nm) was measured after 30 min. The fluorescence spectra were corrected for buffer−TNS contributions.

Analytical Gel Filtration. Analytical gel-filtration chromatography was performed at 22 °C using a TSKgel G3000SW$_{XL}$ (TOSOH Bioscience; LLC Japan) column and a Prostar HPLC system (Varian, Inc.). The column was calibrated with TN buffer containing a mixture of molecular-mass standards [thyroglobulin, 660 kDa; γ-globulin, 165 kDa; ovalbumin, 43 kDa; carbonic anhydrase, 30 kDa; RNAse A, 12.5 kDa; *N*-acetyltryptophanamide (NATA), 0.25 kDa]. CT (2 μM) was run in SN buffer, TN buffer with 1 mM DTA, or TN buffer with 1 M TMAO, and the elution was monitored by the absorbance at 215 nm. The hydrodynamic radius (Stokes radius) and hydrodynamic volume were calculated as described by Uversky (*21*) and are shown in Table 2.

Partial Proteolysis. Limited proteolysis with trypsin was performed by adding 0.0025 mg of trypsin to a 20 μL solution of 2 μM CT in TN buffer, TN buffer with 1 mM DTA, TN buffer with 1 M TMAO, or TN buffer with 30% TFE. Because of the reduced efficacy of trypsin at low pH, we did not perform trypsin cleavage at pH 4 to compare with other conditions. The cleavage reaction was stopped by adding 4× Laemmli sample buffer and boiling for 5 min. The cleaved products were analyzed by SDS−PAGE on a 12% gel.

RESULTS

Prediction of Disorder in HSF1 and Its C-Terminal Regulatory and Activation Domains (CT). We applied PONDR to predict the degree of disorder in HSF1 and CT (Figure 1). This program was developed from the neural network predictors using nonlinear models to estimate any disorder region within a given amino acid sequence. The *x* axis in Figure 1 shows the residue number, whereas the *y* axis is the PONDR score normalized to be 0−1. Any region that exceeds a score of 0.5 is considered disordered. The data show that the PONDR score of the DNA-binding domain (residue 16−80) is 0, indicating a very highly structured segment and supporting the resolved X-ray structure of the DNA-binding domain of the HSF1 homologue in yeast (*33*). The PONDR score of the trimerization domain is below 0.5, indicating a mostly ordered structure. Although no 3D structure of this region has been reported,

the trimerization domain has been well-characterized to form a coil-coiled helical structure within the HSF1 trimer (*5*).

Intriguingly, the longest stretches with the highest PONDR scores reside in the regulatory domain and to a lesser extent in the activation domain. The prediction that the regulatory and activation domains are largely disordered implies that these two domains contain highly flexible segments, which is consistent with the known difficulty in obtaining the X-ray or NMR structure for these domains. The prediction from PONDR encouraged us to further characterize CT.

CD Studies of CT. A number of biochemical and biophysical techniques were used for experimental testing to compare the PONDR neural network-based prediction. CD spectroscopy was performed to determine the secondary- and tertiary-structure components of CT. Similar to several papers showing that intrinsically unstructured proteins display a very low abundance of secondary and tertiary structure (*19*−*21*, *23*, *25*), the CD spectra revealed that CT possesses an extended structure with little secondary or tertiary structure. The far-UV CD spectrum at pH 7 (Figure 2a and Table 1) revealed that the random coil is the major component (*45*). In the near-UV CD spectra, the weak signal at pH 7 also indicated no tertiary structure in CT (Figure 2b).

We next attempted to investigate the conformational alteration of CT by introducing conditions known to induce protein folding. Low pH, the helix-stabilizing TFE (*46*), the osmolyte TMAO, and a cationic surfactant DTA were chosen because each of these has been shown to modify and/or rearrange the protein conformation (*47*−*51*). These experiments revealed that, at pH 4 and lower, the CD spectra were similar to each other. Thus, we chose pH 4 as the acidic condition. The presence of 1 mM DTA maximally induces the secondary structure in CT, and this concentration is lower than the critical micelle concentration (cmc) of DTA (2 mM, data not shown). We found that the CD spectra of CT were similar in 1, 2, or 3 M of the osmolyte TMAO. Thus, we chose 1 M TMAO for our studies. Last, incubation of CT with 30% TFE and higher concentrations gave similar CD spectra. Thus, a concentration of 30% TFE was used in our study.

A clear increase in α-helical content, as revealed by the spectra minima at 208 and 222 nm (*45*), was observed at pH 4, 1 mM DTA, and 1 M TMAO, indicating the induction of the secondary structure in CT (Figure 2a). TFE (30%) most effectively induced the secondary structure.

A quantitative analysis of the induction of the secondary structure in CT was done using CDPro software with the CONTINLL algorithm (*44*). The results summarized in Table 1 show that CT had the greatest amount of secondary structure in 30% TFE (51.4% α helix, 6.5% β strand, and 21.4% turns). At pH 4 or in the presence of 1 mM DTA, the α-helical component of CT is 33.2 and 35.4%, respectively. On the other hand, the presence of 1 M TMAO induced the β-strand component to be 25.5%. All of the conditions demonstrated a clear increase in secondary-structure components as compared to CT under the physiological condition (pH 7) or to the predicted values from SOPMA and GOR IV secondary-structure prediction (*52*, *53*).

In contrast to an induction of the secondary structure under all of the mentioned conditions, the tertiary structure is only evident at pH 4, as reflected by the clear band at 270−280 nm (Figure 2b). This band is attributed to changes in the local environments of the tyrosine residues of CT, suggesting tertiary-structure formation.

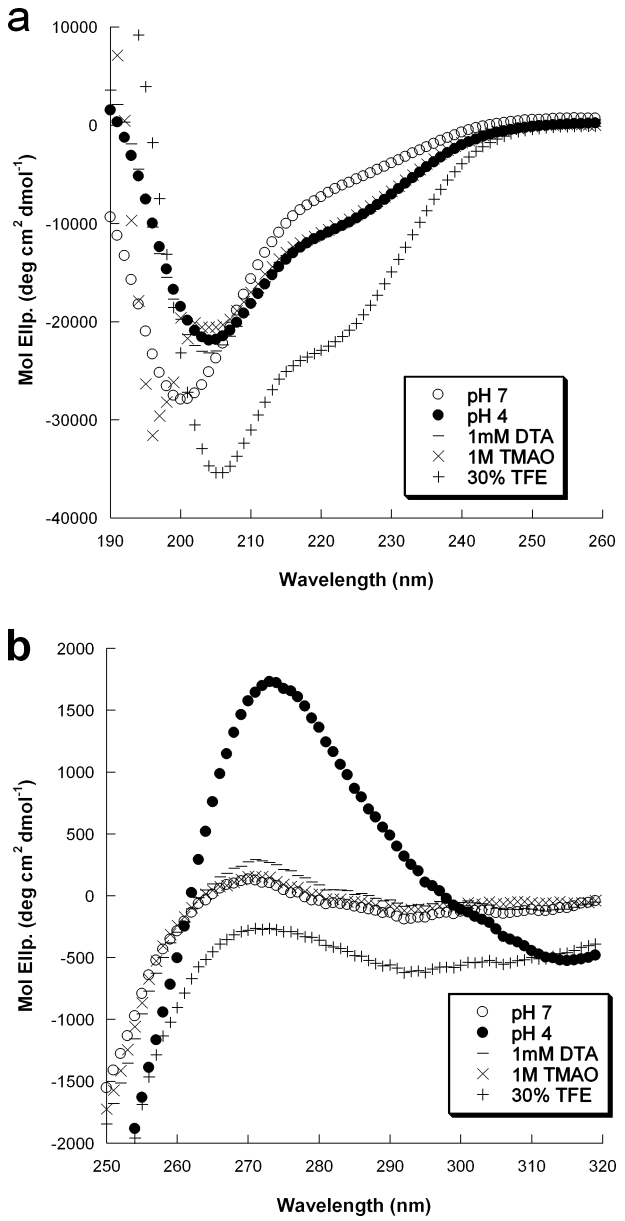

FIGURE 2: CD spectra of CT under different conditions. (a) Far-UV and (b) near-UV. CT (10 μM, in far-UV CD) and CT (3 μM, in near-UV CD) were incubated in TN buffer at pH 7 (○), SN buffer at pH 4 (●), TN buffer containing 1 mM DTA at pH 7 (−), TN buffer containing 1 M TMAO at pH 7 (×), and TN buffer containing 30% TFE at pH 7 (+) at 25 °C for 1 h. The spectra were recorded with a Jasco J-715 spectropolarimeter with an optical path length of 0.01 cm for the far-UV region (190−260 nm) and 0.1 cm for the near-UV region (250−320 nm).

Intrinsic Fluorescence of CT. Intrinsic tyrosine fluorescence was used to follow the conformational changes of CT using an excitation wavelength of 274 nm (*54*) and monitoring the emission spectrum from 290 to 350 nm. The quantum yield of tyrosine is sensitive to changes in its local environment, resulting in a change in the fluorescence intensity.

The fluorescence of CT was found to be highest in the presence 30% TFE and lowest in the presence of 1 M TMAO (Figure 3), while the signals are comparable at pH 7, pH 4, and 1 mM DTA. The emission maximum is at 303 nm in 30% TFE and at 305 nm under all other conditions. The slight Stokes shift toward a shorter wavelength in the

Table 1: CT Secondary-Structure Composition at Various Conditions as Estimated Using the Far-UV CD Spectral Data[a]

conditions	α helix (%)	β sheet (%)	turn (%)	unordered (%)
pH 7	22.4	10.8	26.2	40.6
pH 4	33.2	7.2	25.9	33.7
1 mM DTA	35.4	6.9	25.0	32.8
1 M TMAO	17.3	25.5	17.3	40.0
30% TFE	51.4	6.5	21.4	20.7
predicted values[b]	17.9	13.4	3.8	65.0[c]
predicted values[d]	11.3	14.5	N/A	75.0[c]

[a] Values were calculated using CDPro. [b] Estimated from the secondary-structure prediction using the SOPMA algorithm available at the SOPMA SECONDARY STRUCTURE PREDICTION METHOD server (*52*). [c] The value is for non-α-helical and non-β-strand regions. [d] Estimated from the secondary-structure prediction using the GOR IV algorithm available at the GOR IV SECONDARY STRUCTURE PREDICTION METHOD server (*53*).

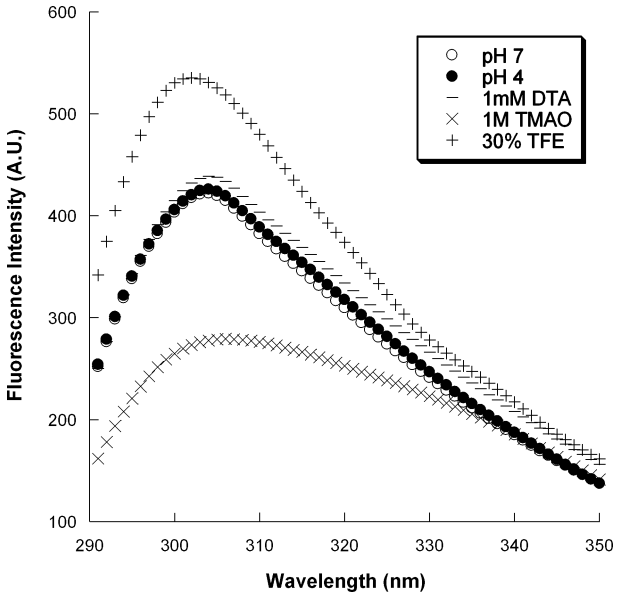

FIGURE 3: Intrinsic fluorescence of CT under different conditions. CT (2 μM) was incubated in TN buffer at pH 7 (○), SN buffer at pH 4 (●), TN buffer containing 1 mM DTA at pH 7 (−), TN buffer containing 1 M TMAO at pH 7 (×), and TN buffer containing 30% TFE at pH 7 (+), respectively. Fluorescence was measured after 30 min of incubation at 22 °C by an FP-6500 spectrofluorometer, with an excitation wavelength of 274 nm.

presence of 30% TFE is likely the result of the less polar environment (*46*). The substantial changes seen in CT fluorescence in the presence of TFE and TMAO may largely originate from the solvent effects, with the less polar environment in the TFE aqueous solution increasing the quantum yield of tyrosine residues, while TMAO has a quenching effect, leading to a decrease in tyrosine fluorescence.

Determination of CT Hydrophobic Domain Formation. One characteristic of a natively unfolded protein is a lack of hydrophobic clusters. The hydrophobic probe TNS was used to monitor the hydrophobicity of CT. This probe has a low fluorescence quantum yield in a polar environment, such as water, and the quantum yield significantly increases when the probe is in a nonpolar environment. TNS fluorescence was nearly 0 when CT was incubated at neutral pH (pH 7.4), in the presence of 1 M TMAO, or in 30% TFE, indicating that CT lacks hydrophobic clusters under these conditions (Figure 4). At pH 4 or in the presence of 1 mM DTA,

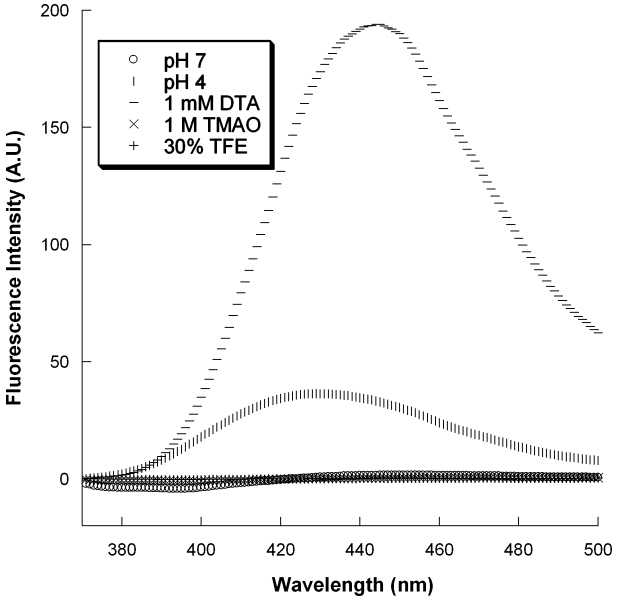

FIGURE 4: Fluorescence emission spectra of TNS bound to CT under different conditions. CT (2 μM) was incubated in TN buffer at pH 7 (○), SN buffer at pH 4 (|), TN buffer containing 1 mM DTA at pH 7 (−), TN buffer containing 1 M TMAO at pH 7 (×), and TN buffer containing 30% TFE at pH 7 (+), respectively. TNS (20 μM) was added after 1 h of incubation at 22 °C, and the fluorescence was measured after 30 min by the FP-6500 spectrofluorometer, with an excitation wavelength at 310 nm.

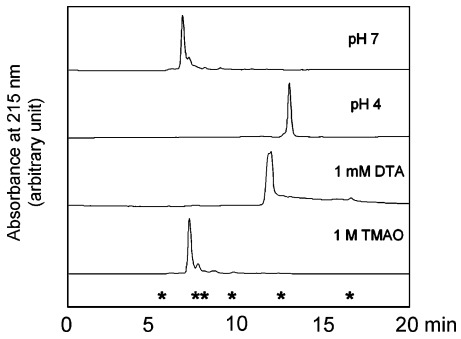

FIGURE 5: Size-exclusion HPLC of CT under different conditions. CT (2 μM) was incubated in TN buffer at pH 7.4 (panel 1), SN buffer at pH 4 (panel 2), TN buffer containing 1 mM DTA at pH 7.4 (panel 3), and TN buffer containing 1 M TMAO at pH 7.4 (panel 4) for 20 min and run in the same mobile phase as in the incubation condition. The absorbance at 215 nm was recorded.

however, TNS fluorescence increases by 40- and 190-fold, respectively, indicating the presence of hydrophobic clusters in CT.

The observation that the cationic detergent DTA is more effective than acidic pH in increasing TNS fluorescence does not necessarily reflect a more pronounced effect of DTA in inducing the formation of hydrophobic clusters in CT. We believe that the fluorescence increase at 1 mM DTA may be largely attributable to a CT−DTA complex that creates a micelle-like environment, i.e., a protein-facilitated formation of DTA micelles.

Size-Exclusion HPLC of CT. The degree of compactness of CT was used as an indicator of the collapse to a globular structure. When CT migrated in a size-exclusion column, it eluted fastest at pH 7.4 and slowest at pH 4 (Figure 5). When CT both at pH 7.4 and in the presence of 1 M TMAO was compared to the molecular-weight markers that were run under the same conditions, it eluted with a molecular weight

Table 2: Calculated and Measured Stokes Radii (Rs) and Hydrodynamic Volumes (Vh) of CT[a]

	measured		calculated folded		calculated unfolded	
conditions	Rs (Å)	Vh (Å^3)	Rs(N)[b] (Å)	Vh(N)[c] (Å^3)	Rs(U)[d] (Å)	Vh(U)[e] (Å^3)
pH 7.4	38.4	237 062	25.1	68 865	51.3	487 429
pH 4	15.8	16 153				
1 mM DTA	18.5	26 508				
1 M TMAO	38.2	233 377				

[a] The abbreviations used are as follows: N, native; U, unfolded; MW, molecular weight (in daltons); *n*, number of amino acid residues. [b] Log Rs(N) = 0.369 log(MW) − 0.254. [c] Log Vh(N) = (2.197 ± 0.037) + (1.072 ± 0.015)log *n*. [d] Log Rs(U) = 0.533 log(MW) − 0.682; $V = 4/3\pi$Rs3. [e] Log Vh(U) = (1.997 ± 0.078) + (1.498 ± 0.035)log *n*.

of 165 kDa, about 5 times greater than its calculated molecular weight of 31 kDa. At pH 4 or in the presence of 1 mM DTA, on the other hand, CT eluted at the volume corresponding to a molecular weight of 12.5−30 kDa. Acidic pH and the cationic surfactant thus induce the CT structure to collapse into a much smaller particle than at neutral pH or in the presence of the osmolyte TMAO. We were unable to perform an experiment using TFE as the mobile phase because buffer containing TFE created a high volume of air bubbles, which could not be completely degassed in the HPLC system.

The elution volumes of CT under different conditions were used to calculate the Stokes radii and the hydrodynamic volumes assuming a spherical particle. The column was calibrated using a set of protein standards of known Stokes radii, and the results are summarized in Table 2. The data set from SEC was compared to the values calculated from the amino acid sequence according to Uversky (*21*), who employed a set of native globular proteins and Gdn-HCl-denatured proteins to create a correlation between the measured Stokes radii from SEC and the molecular weight of the proteins.

The theoretically calculated Stokes radius and the hydrodynamic volume of folded CT are about 25 Å and 69 000 Å^3, respectively, whereas those of unfolded CT are about 51 Å and 490 000 Å^3, respectively (Table 2). Our measured data show that CT at pH 7.4 and in the presence of 1 M TMAO is an extended molecule and has a hydrodynamic volume of half the size of that calculated for fully unfolded CT. In contrast, the CT structure was quite compact under acidic conditions and in the presence of a cationic detergent, giving Stokes radii of about 16 and 19 Å and hydrodynamic volumes of about 17 000 and 27 000 Å^3, respectively. The significantly reduced size of CT at pH 4 and 1 mM DTA as compared to that predicted for a globular structure (*21*) suggests that folded CT is very compact.

Limited Proteolysis of CT. Natively unfolded proteins are very susceptible to enzymatic cleavage because of their flexible structure (*55*), while well-folded proteins are more resistant to proteolysis. Limited proteolysis thus allows one to probe the degree of the unfolded state and determine which parts of the polypeptide chain are protected. Trypsin was used as the proteolytic enzyme in this study taking advantage of the relatively even distribution of the cleavage sites within the CT sequence. The trypsin concentration was adjusted to give the same activity under each condition by using the synthetic substrate *p*-toluene-sulfonyl-L-arginine methyl ester (TAME) as a standard to correct for the effects of the agents contained in the buffer.

The results show that the intact CT band disappeared within 2 min after adding trypsin, giving fragments between 25 and 35 kDa (lane 3 in Figure 6) and possibly smaller fragments that were not detected. At pH 7.9 and in the presence of 1 M TMAO, the main 27 kDa fragment persisted at 5 min of trypsin cleavage and gradually disappeared (lanes 4−6 and 12−14 in Figure 6, respectively). However, in the presence of 1 mM DTA or 30% TFE, the 27−35 kDa fragments of CT were resistant to trypsin even after 30 min (triangle marks in lanes 8−10 and 16−18 in Figure 6, respectively). The presence of 30% TFE most effectively protected CT from tryptic digestion, giving the three main fragments at 27−35 kDa (triangle marks). The results suggest that the presence of a cationic surfactant or TFE induce the rearrangement of the CT structure, protecting the trypsin cleavage sites from proteolysis.

The proteolytic sensitivity of CT was also determined with the Glu-C endroproteinase from the *Staphlococcus aurius* strain V8 (V8 endoproteinase), which cleaves on the C side of glutamic and aspartic acid residues. Surprisingly, similar results were found with the trypsin cleavage experiment. In the V8 cleavage, the 27 kDa fragment was also produced in the presence of 1 mM DTA or 30% TFE (data not shown). Although the proteolytic attack of CT by trypsin and V8 endoproteinase occurs at different sites, they both gave similar fragments, suggesting protease-independent resistance of "folded CT".

Unfolding Studies of CT. To assess the conformational stability of CT in its native and induced-folded form, heat-induced unfolding and Gdn-HCl denaturation were performed and the denaturation was followed by far-UV CD. We chose the conditions that were most effective in inducing CT folding as observed by changes in secondary-structure content, hydrophobicity, and hydrodynamic properties, namely, the acidic condition and the presence of the cationic detergent, DTA.

The ellipticity at 222 nm, a characteristic of α-helical content (*56*), was measured as a function of the temperature. At pH 7, the magnitude of the molar ellipticity increases from −3200 to −4500° cm^2 dmol^{-1} in the 20−80 °C scan, indicating an increase in the helical component with temperature (Figure 7). The reversed temperature scan of the same sample (80−20 °C) shows the magnitude of the ellipticity decreasing from −4400to −3000° cm^2 dmol^{-1}, suggesting that the temperature-induced conformational change of CT is reversible (Figure 7). It is noteworthy that no cooperative folding of CT was observed; i.e., the changes in secondary-structure content were monotonous in both the forward and reverse temperature scans.

CT at pH 4 or in the presence of 1 mM DTA exhibits higher helical structure content compared to that at pH 7, with a molar ellipticity of −5300 and −5700° cm^2 dmol^{-1}, respectively (Figure 7). The temperature scan at pH 4 caused a gradual increase in the ellipticity of CT until the sample reached 60 °C, indicating a small induction of helical content. The ellipticity drastically declined from 60 to 80 °C because of the precipitation of the protein. In the presence of 1 mM DTA, a small change in the ellipticity indicated that the

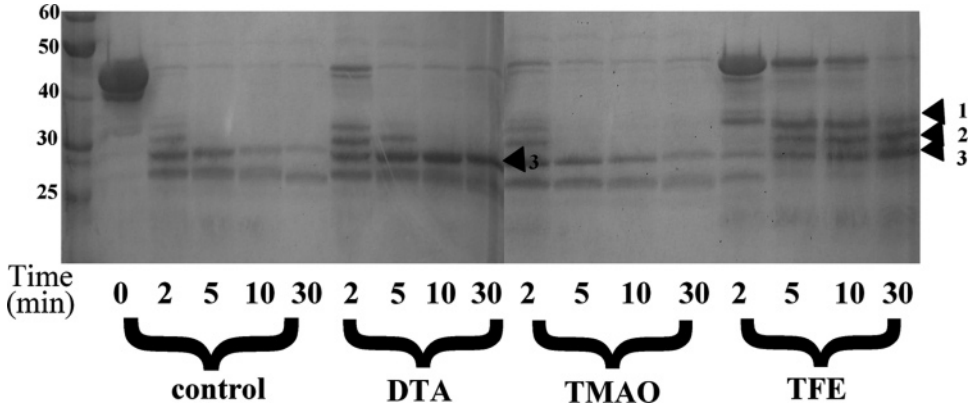

FIGURE 6: Limited proteolysis of CT under different conditions. CT (10 μM) was incubated at normal condition (10 mM Tris at pH 7.9, lanes 2−6), in 1 mM DTA (lanes 7−10), 1 M TMAO (lanes 11−14), and 30% TFE (lanes 15−18). The cleavage reaction was started by the addition of 0.0025 μg of trypsin to the samples. The reaction was stopped at 2, 5, 10, and 30 min with SDS loading buffer and boiling at 100 °C for 5 min. The cleaved samples were separated with SDS−PAGE.

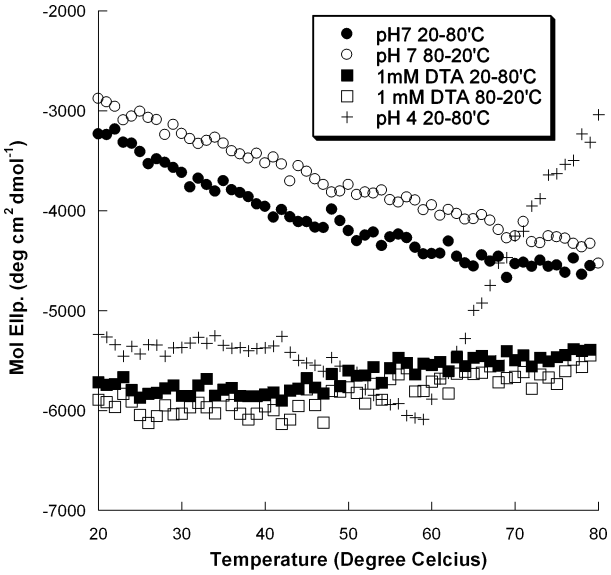

FIGURE 7: $CD_{222\ nm}$ of CT as a function of the temperature. CT (3 μM) was incubated in TN buffer at pH 7 (●, 20−80 °C; ○, 80−20 °C), TN buffer containing 1 mM DTA at pH 7 (■, 20−80 °C; □, 80−20 °C), or SN buffer at pH 4 (+, 20−80 °C) for 1 h. The spectra were recorded with a Jasco J-715 spectropolarimeter equipped with a temperature control unit, with an optical path length of 1 mm. The samples were scanned with increased and decreased temperature in the range of 20−80 °C. The increment time was 60 °C/h.

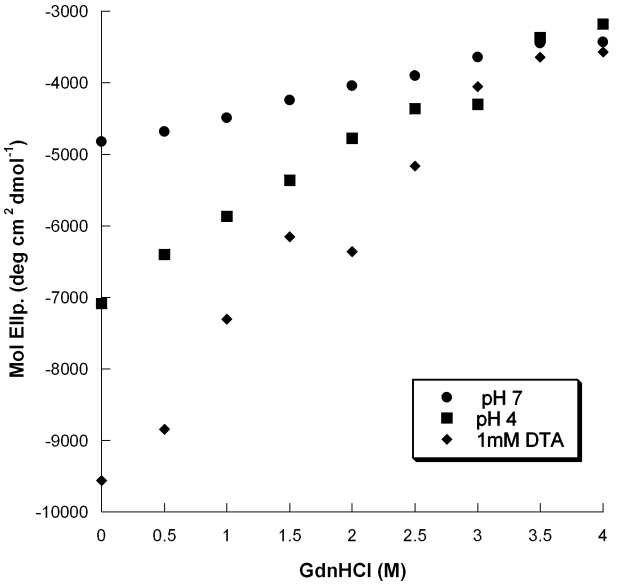

FIGURE 8: $CD_{222\ nm}$ of CT as a function of GdnHCl under different conditions. CT (3 μM) was incubated in TN buffer at pH 7 (●), SN buffer at pH 4 (■), or TN buffer containing 1 mM DTA at pH 7 (◆) for 1 h. GdnHCl was added to the samples to final concentrations of 0.5−4 M.

conformation of CT was marginally influenced by the temperature.

Gdn-HCl denaturation was performed to determine the stability of the induced-folded conformation of CT. The steeper slope of the ellipticity seen in the presence of 1 mM DTA as compared with that at pH 4 and 7 when the concentration of Gdn-HCl increases indicates greater changes in secondary components of CT (Figure 8). At 3.5 M Gdn-HCl, CT exhibits a similar ellipticity under all conditions, showing that Gdn-HCl can unfold the folded structure of CT to an extended conformation under all conditions applied. No secondary structure was found when analyzing the CD spectra of CT in 3.5 M Gdn-HCl, suggesting that this concentration can completely unfold the CT structure.

DISCUSSION

The protein structure function paradigm states that a well-defined folded structure is a prerequisite for a protein to be functional. More recently, however, the complementary view has been expressed that the unfolded structure can be assigned function as well. The accumulating evidence for the interplay between the protein disorder and biological role emphasizes that native disorder is a common phenomenon in the eukaryotic genome and that as many as 30% of proteins in eukaryotic cells may be natively unfolded (*23*), with more than 30 types of potential functions (*57*). Generally speaking, functions of natively unfolded proteins originate either from their ability to fluctuate freely in conformational space or their ability to transiently or permanently interact with their biological partners (*22*).

Recent studies indicate that large regions within several gene-specific transcription factors are natively unfolded (*58*−*65*). This feature may enable these proteins to interact with a large number of partners during the transcriptional activation/deactivation process. The partners vary from post-translational modifiers (*66*), chaperones (*67*), general transcription factors (*68*, *69*), chromatin-remodeling proteins (*70*), and transcriptional mediators (*71*). Playing a key role

Table 3: Major Characteristics of HSF1 and Its N- and C-Terminal Parts[a]

domain	length (amino acids)	M_r (Da)	pI	net charge	mean net charge	hydrophobicity[b] total	hydrophobicity[b] mean
full-length HSF1	503	54 930.80	5.24	−18	0.0358	225.584	0.4521
N-termial part of HSF1	212	24 172.10	9.46	8	0.0377	95.382	0.4585
C-terminal part of HSF1	291	30 776.70	4.34	−26	0.0893	127.649	0.4448
C-terminal part of HSF1 at pH 4	291	30 776.70	N/A	−8	0.0275	127.649	0.448

[a] All calculations were taken from the server ExPASy amino acid sequence analysis ProtParam and ProtScale. [b] The hydrophobicity was calculated by the Kyte and Doolittle approximation.

as a gene-specific transcription factor in heat-shock genes, HSF1 can also be expected to contain regions that are natively disordered. In this study, we provide evidence that CT is indeed largely unfolded at physiologic pH but can be induced to fold under certain conditions.

Native Disorder of CT. CT encompasses the regulatory and transcriptional activation domains. It plays a critical role in the molecular recognition and undergoes post-translational modifications as part of the HSF1 activation/deactivation pathway. Our study demonstrates that CT displays the structural characteristics that define unfolded proteins (*19*−*21*, *23*, *72*): (1) a very low abundance of secondary and tertiary structures, (2) an absence of a hydrophobic core, (3) a large hydrodynamic size, and (4) a high structural flexibility.

Recent studies have suggested that natively unfolded proteins can be distinguished from globular proteins with a high confidence based on their amino acid sequences (*21*, *23*, *72*, *73*). Results of the sequence analysis done in this study indeed supports the assignment of native disorder to CT and is also in agreement with the prediction from the neural-network-based PONDR. Moreover, the charge calculation using the ExPaSy server (*74*, *75*) indicated that CT has a highly uncompensated net charge under physiologic conditions when compared with the full-length HSF1 or with the N terminus of HSF1 (residues 1−212) (Table 3). Also, the amino acid composition of CT is low in hydrophobic residues and significantly depleted in order-promoting amino acids (W, C, F, I, Y, V, L, and N, 25.4%), while it is enriched in charged and disorder-promoting amino acids (A, R, G, Q, S, P, E, and K, 54.9%). In particular, the high prevalence of negatively charged residues in CT promotes extension of the peptide chain, inhibiting the formation of a collapsed globular structure.

Serine is the most abundant amino acid in the CT sequence (16.5%). It is known that the major phosphorylation sites of HSF1 reside in the CT region (*17*); thus, it is possible that the high percentage of serine residues indicates a role for disorder in protein phosphorylation. Indeed, lacking a defined structure may allow multiple phosphorylation of a protein segment by different kinases. Iakoucheva et al. (*76*) also pointed out that, in the SWISS-PROT protein database, disorder-promoting residues tend to surround phosphorylation sites. Our results are in line with this observation. It is interesting to note that proline is the second most abundant residue in the CT sequence (12.7%). While not charged, proline is known to be a helix breaker (*77*), and its high abundance in CT as compared with the 5.2% average occurrence of proline in proteins (*78*, *79*) might play a critical role in destabilizing the secondary structure and promoting a disordered structure.

While the results of the current study indicate that CT is natively largely unfolded, it needs to be noted that in intact HSF1 the leucine zipper LZ4 located within the CT domain (Figure 1) interacts with the leucine zippers LZ1−LZ3 in the trimerization domain (*9*). This intramolecular interaction has been proposed to play an important regulatory role, keeping HSF1 in its inactive monomeric form. It is possible that, in the full-length protein, this interaction might contribute to the acquisition of some structure in the CT domain.

Environmental Effects in the Induced Folding of CT. In light of the evidence suggesting that CT is natively largely unfolded, an important question is whether this protein segment can be induced to fold. Several conditions known to promote protein folding were applied to test this possibility, and the conformational changes were monitored using a number of biochemical and biophysical approaches. Four conditions known to induce secondary-structure formation were chosen; acidic pH (*47*, *48*, *80*, *81*), a cationic detergent DTA (*51*), an osmolyte TMAO (*50*, *60*, *82*), and an organic solvent TFE (*49*, *82*, *83*). Overall, the results suggest that all conditions could induce structure in CT to some extent, as observed by CD spectroscopy (Figure 2a).

Low pH as well as DTA induced a collapse of CT to a compact structure with a hydrophobic core (Figures 4 and 5). However, while incubation at pH 4 induced both secondary and tertiary structures, DTA only significantly induced the secondary structure, with only small effects on the tertiary structure (parts a and b of Figure 2). While TFE also induced the secondary structure (Figure 2a), it failed to produce the tertiary structure or hydrophobic clusters in CT (Figures 2b and 4). It is known that TFE stabilizes the α helix in proteins, probably by increasing intrapeptide hydrogen bonding and also by enhancing the favorable interaction between hydrophobic side chains and TFE (*84*). However, the secondary structure induced by TFE has been found irrelevant biologically because this reagent does not preferentially support the correct α helices (*85*).

TMAO was found to have the mildest effect on the CT structure. While TMAO enhanced the α-helical content, it did not induce the folding of CT to a compact structure with hydrophobic clusters (Figures 4 and 5). TMAO is known to be an effective osmolyte that stabilizes the folded states of proteins possibly via the interaction between TMAO and the peptide backbone (*60*, *86*).

Limited proteolysis was performed to further characterize the structural alterations in CT under the conditions mentioned above. The results show that either 1 mM DTA or 30% TFE reduced the rate of trypsin cleavage of CT such that the large cleaved fragments still remained intact after 30 min. This suggests that both DTA and TFE alter CT

conformation, creating domains that are resistant to tryptic digestion.

The protease resistance of CT in the presence of DTA seemed to arise from a different origin than the one seen in TFE. The physicochemical data suggest that CT was induced to fold to a compact structure with a collapsed hydrophobic core in the presence of DTA, but none of those happened in the presence of TFE. The mechanism by which TFE can enhance structure formation in a protein is by excluding water molecules from surrounding the polypeptide chain through hydrogen bonding, resulting in a less polar local environment (*84*). Under such conditions, the random coil of CT is induced to acquire the secondary structure through the formation of intrachain hydrogen bonds.

The surfactant DTA acts in a different manner. In addition to interacting with hydrophobic groups in the polypeptide chain, the positive charges of DTA electrostatically interact with the negatively charged side chains on the acidic CT molecule, thereby reducing intrachain repulsion and allowing the collapse of the molecule to a more compact structure. Charge neutralization thus allows hydrophobic interactions in CT to facilitate this collapse to a compact structure. In addition, it is likely that DTA also acts as a surfactant and creates a nonpolar, membrane-like environment for CT that promotes folding and hydrophobic core formation.

Temperature elevation was found to induce the secondary structure in CT, and this effect is reversible (Figure 7). The gradual increase in the magnitude of the molar ellipticity as the temperature increases indicates the non-cooperative induction of the α-helical content. This non-cooperative temperature induction is typical of natively unfolded proteins and is believed to reflect their conformational flexibility. The induced secondary structure is believed to result from enhanced hydrophobic interactions between amino acid side chains at high temperatures (*21*).

Functional Implications of the Natively Unfolded and Induced-Folded State of CT. CT contains both the regulatory and activation domains of HSF1. During the dynamic process of the heat-shock response, HSF1 becomes post-translationally modified and transiently interacts with several biological partners in a timely manner. CT, as an integral component in these interactions, needs to undergo major structural changes as well. Being natively unfolded, CT has the ability to adopt a number of defined structures (*25*, *29*). This flexibility may allow for the transcription factor to quickly respond to chemical modifications, such as phosphorylation/dephosphorylation or small ubiquitin-related modifier (SUMO)ylation, during the heat-shock-induced activation/deactivation process (*25*, *87*). We further suggest that the largely disordered structure of CT may allow HSF1 to interact with several proteins in a transient manner and that these short-lived protein−protein interactions are characterized by high specificity (because CT changes conformation specifically to fit one of a few partners but not any protein) but low affinity (because the flexibility of CT lowers the free energy of the interaction) and may in fact control Hsp gene expression by allowing it to be a rapid process, as needed for cell survival.

Both the regulatory and activation domains of HSF1 have been reported to interact with a multichaperone complex Hsp90−p23−FKBP52 (*13*, *88*), as well as with Hsp70 (*89*). These chaperones are known to interact with nascent proteins that are not fully folded. The observation that the CT domain of HSF1 is largely unfolded supports this assertion. Moreover, it has been proposed that the multichaperone complexes regulate the heat-shock activation/deactivation pathway in which the chaperones and co-chaperones dissociate from HSF1, thereby allowing for the structural transition of HSF1 to the active form (*12*). We hypothesize that the unfolded CT region of HSF1 can be structurally modulated by the associated multichaperone complex to gain structural elements that affect the whole HSF1 structure and induce it to readily assemble to a trimer or disintegrate to a monomer. Evidence of HSF1 structural modulation by the multichaperone complex is needed to support this hypothesis.

The induced folding of CT documented in this study implies that this region of HSF1 may undergo a disorder−order transition upon binding to its biological partners. It has been reported that the TATA-binding protein (TBP) can induce the folding of the glucocorticoid receptor AF1/tau1 domain (*50*, *90*) and the estrogen receptor (*91*), resulting in increased secondary-structure content. TBP, reported to interact with the CT region of HSF1 (*11*, *92*), might induce the folding of unstructured CT, leading it to acquire the secondary and/or tertiary structure. Such an induced-folded structure may play an important role in modulating the molecular recognition between HSF1 and its partners, as well as modifying the HSF1−DNA interaction. The TBP-binding-induced folding of CT would thus be of great interest for further investigations.

ACKNOWLEDGMENT

The authors thank Dr. Dennis Thiele (Pharmacology and Cancer Biology, Duke University Medical Center, Durham, NC) for the full-length plasmid cDNA of mouse HSF1.

REFERENCES

1. Christians, E. S., Yan, L. J., and Benjamin, I. J. (2002) Heat shock factor 1 and heat shock proteins: Critical partners in protection against acute cell injury. *Crit. Care Med. 30*, S43−S50.
2. Mathew, A., Shi, Y., Jolly, C., and Morimoto, R. I. (2000) Analysis of the mammalian heat-shock response. Inducible gene expression and heat-shock factor activity, *Methods Mol. Biol. 99*, 217−255.
3. Trinklein, N. D., Murray, J. I., Hartman, S. J., Botstein, D., and Myers, R. M. (2004) The role of heat shock transcription factor 1 in the genome-wide regulation of the mammalian heat shock response, *Mol. Biol. Cell 15*, 1254−1261.
4. Sorger, P. K. (1991) Heat shock factor and the heat shock response, *Cell 65*, 363−366.
5. Wu, C. (1995) Heat shock transcription factors: Structure and regulation, *Annu. Rev. Cell Dev. Biol. 11*, 441−469.
6. Cotto, J. J., and Morimoto, R. I. (1999) Stress-induced activation of the heat-shock response: Cell and molecular biology of heat-shock factors, *Biochem. Soc. Symp. 64*, 105−118.
7. Pirkkala, L., Nykanen, P., and Sistonen, L. (2001) Roles of the heat shock transcription factors in regulation of the heat shock response and beyond, *FASEB J. 15*, 1118−1131.
8. Morimoto, R. I. (1998) Regulation of the heat shock transcriptional response: Cross talk between a family of heat shock factors, molecular chaperones, and negative regulators, *Genes Dev. 12*, 3788−3796.
9. Rabindran, S. K., Haroun, R. I., Clos, J., Wisniewski, J., and Wu, C. (1993) Regulation of heat shock factor trimer formation: Role of a conserved leucine zipper, *Science 259*, 230−234.
10. Lis, J., and Wu, C. (1993) Protein traffic on the heat shock promoter: Parking, stalling, and trucking along, *Cell 74*, 1−4.
11. Yuan, C. X., and Gurley, W. B. (2000) Potential targets for HSF1 within the preinitiation complex, *Cell Stress Chaperones 5*, 229−242.

12. Morimoto, R. I. (2002) Dynamic remodeling of transcription complexes by molecular chaperones, *Cell 110*, 281−284.
13. Guo, Y., Guettouche, T., Fenna, M., Boellmann, F., Pratt, W. B., Toft, D. O., Smith, D. F., and Voellmy, R. (2001) Evidence for a mechanism of repression of heat shock factor 1 transcriptional activity by a multichaperone complex, *J. Biol. Chem. 276*, 45791−45799.
14. Hong, Y., Rogers, R., Matunis, M. J., Mayhew, C. N., Goodson, M. L., Park-Sarge, O. K., and Sarge, K. D. (2001) Regulation of heat shock transcription factor 1 by stress-induced SUMO-1 modification, *J. Biol. Chem. 276*, 40263−40267.
15. Park, J., and Liu, A. Y. (2001) JNK phosphorylates the HSF1 transcriptional activation domain: Role of JNK in the regulation of the heat shock response, *J. Cell. Biochem. 82*, 326−338.
16. Sullivan, E. K., Weirich, C. S., Guyon, J. R., Sif, S., and Kingston, R. E. (2001) Transcriptional activation domains of human heat shock factor 1 recruit human SWI/SNF, *Mol. Cell. Biol. 21*, 5826−5837.
17. Holmberg, C. I., Tran, S. E. F., Eriksson, J. E., and Sistonen, L. (2002) Multisite phosphorylation provides sophisticated regulation of transcription factors, *Trends Biochem. Sci. 27*, 619−627.
18. Hu, Y. Z., and Mivechi, N. F. (2003) HSF-1 interacts with Ral-binding protein 1 in a stress-responsive, multiprotein complex with HSP90 in vivo, *J. Biol. Chem. 278*, 17299−17306.
19. Tompa, P. (2002) Intrinsically unstructured proteins, *Trends Biochem. Sci. 27*, 527−533.
20. Uversky, V. N. (2002) Natively unfolded proteins: A point where biology waits for physics, *Protein Sci. 11*, 739−756.
21. Uversky, V. N. (2002) What does it mean to be natively unfolded? *Eur. J. Biochem. 269*, 2−12.
22. Tompa, P. (2005) The interplay between structure and function in intrinsically unstructured proteins, *FEBS Lett. 579*, 3346−3354.
23. Fink, A. L. (2005) Natively unfolded proteins, *Curr. Opin. Struct. Biol. 15*, 35−41.
24. Iakoucheva, L. M., Brown, C. J., Lawson, J. D., Obradovic, Z., and Dunker, A. K. (2002) Intrinsic disorder in cell-signaling and cancer-associated proteins, *J. Mol. Biol. 323*, 573−584.
25. Radivojac, P., Obradovic, Z., Smith, D. K., Zhu, G., Vucetic, S., Brown, C. J., Lawson, J. D., and Dunker, A. K. (2004) Protein flexibility and intrinsic disorder, *Protein Sci. 13*, 71−80.
26. Gunasekaran, K., Tsai, C. J., Kumar, S., Zanuy, D., and Nussinov, R. (2003) Extended disordered proteins: Targeting function with less scaffold, *Trends Biochem. Sci. 28*, 81−85.
27. Gunasekaran, K., Haspel, N., Tsai, C. J., Kumar, S., Wolfson, H., and Nussinov, R. (2003) Extended disordered proteins: An elegant solution to having large intermolecular interfaces, yet keeping smaller genome and cell sizes, *Biophys. J. 84*, 163A.
28. Bussell, R., and Eliezer, D. (2001) Residual structure and dynamics in Parkinson's disease-associated mutants of α-synuclein, *J. Biol. Chem. 276*, 45996−46003.
29. Fuxreiter, M., Simon, I., Friedrich, P., and Tompa, P. (2004) Preformed structural elements feature in partner recognition by intrinsically unstructured proteins, *J. Mol. Biol. 338*, 1015−1026.
30. Voellmy, R. (1996) Sensing stress and responding to stress, in *Stress-Inducible Cellular Responses* (Feige, U., Morimoto, I., Yahara, I., and Polla, B., Eds.) Vol. *77*, pp 121−137, Birkhauser Verlag, Basel, Switzerland.
31. Morimoto, R. I., Kline, M. P., Bimston, D. N., and Cotto, J. J. (1997) The heat-shock response: Regulation and function of heat-shock proteins and molecular chaperones, *Essays Biochem. 32*, 17−29.
32. Westerheide, S. D., and Morimoto, R. I. (2005) Heat shock response modulators as therapeutic tools for diseases of protein conformation, *J. Biol. Chem. 280*, 33097−33100.
33. Littlefield, O., and Nelson, H. C. M. (1999) A new use for the "wing" of the "winged" helix−turn−helix motif in the HSF−DNA cocrystal, *Nat. Struct. Biol. 6*, 464−470.
34. Cicero, M. P., Hubl, S. T., Harrison, C. J., Littlefield, O., Hardy, J. A., and Nelson, H. C. M. (2001) The wing in yeast heat shock transcription factor (HSF) DNA-binding domain is required for full activity, *Nucleic Acids Res. 29*, 1715−1723.
35. Clos, J., Westwood, J. T., Becker, P. B., Wilson, S., Lambert, K., and Wu, C. (1990) Molecular cloning and expression of a hexameric *Drosophila* heat shock factor subject to negative regulation, *Cell 63*, 1085−1097.
36. Rabindran, S. K., Giorgi, G., Clos, J., and Wu, C. (1991) Molecular cloning and expression of a human heat shock factor, HSF1, *Proc. Natl. Acad. Sci. U.S.A. 88*, 6906−6910.
37. Kroeger, P. E., Sarge, K. D., and Morimoto, R. I. (1993) Mouse heat shock transcription factors 1 and 2 prefer a trimeric binding site but interact differently with the HSP70 heat shock element, *Mol. Cell. Biol. 13*, 3370−3383.
38. Sarge, K. D., Murphy, S. P., and Morimoto, R. I. (1993) Activation of heat shock gene transcription by heat shock factor 1 involves oligomerization, acquisition of DNA-binding activity, and nuclear localization and can occur in the absence of stress, *Mol. Cell. Biol. 13*, 1392−1407.
39. Ahn, S. G., Liu, P. C., Klyachko, K., Morimoto, R. I., and Thiele, D. J. (2001) The loop domain of heat shock transcription factor 1 dictates DNA-binding specificity and responses to heat stress, *Genes Dev. 15*, 2134−2145.
40. Romero, Obradovic, and Dunker, K. (1997) Sequence data analysis for long disordered regions prediction in the calcineurin family, *Genome Inf. Ser. 8*, 110−124.
41. Li, X., Romero, P., Rani, M., Dunker, A. K., and Obradovic, Z. (1999) Predicting protein disorder for N-, C-, and internal regions, *Genome Inf. Ser. 10*, 30−40.
42. Romero, P., Obradovic, Z., Li, X., Garner, E. C., Brown, C. J., and Dunker, A. K. (2001) Sequence complexity of disordered protein, *Proteins 42*, 38−48.
43. Kelly, S. M., Jess, T. J., and Price, N. C. (2005) How to study proteins by circular dichroism, *Biochim. Biophys. Acta 1751*, 119−139.
44. Sreerama, N., and Woody, R. W. (2004) Computation and analysis of protein circular dichroism spectra, *Methods Enzymol. 383*, 318−351.
45. Shi, Z., Woody, R. W., and Kallenbach, N. R. (2002) Is polyproline II a major backbone conformation in unfolded proteins? *Adv. Protein Chem. 62*, 163−240.
46. Starzyk, A., Barber-Armstrong, W., Sridharan, M., and Decatur, S. M. (2005) Spectroscopic evidence for backbone desolvation of helical peptides by 2,2,2-trifluoroethanol: An isotope-edited FTIR study, *Biochemistry 44*, 369−376.
47. Busch, R., Reich, Z., Zaller, D. M., Sloan, V., and Mellins, E. D. (1998) Secondary structure composition and pH-dependent conformational changes of soluble recombinant HLA-DM, *J. Biol. Chem. 273*, 27557−27564.
48. Kumar, D. P., Tiwari, A., and Bhat, R. (2004) Effect of pH on the stability and structure of yeast hexokinase A. Acidic amino acid residues in the cleft region are critical for the opening and the closing of the structure, *J. Biol. Chem. 279*, 32093−32099.
49. Polverino de Laureto, P., Frare, E., Gottardo, R., and Fontana, A. (2002) Molten globule of bovine α-lactalbumin at neutral pH induced by heat, trifluoroethanol, and oleic acid: A comparative analysis by circular dichroism spectroscopy and limited proteolysis, *Proteins 49*, 385−397.
50. Kumar, R., Lee, J. C., Bolen, D. W., and Thompson, E. B. (2001) The conformation of the glucocorticoid receptor af1/tau1 domain induced by osmolyte binds co-regulatory proteins, *J. Biol. Chem. 276*, 18146−18152.
51. Viseu, M. I., Carvalho, T. I., and Costa, S. M. (2004) Conformational transitions in β-lactoglobulin induced by cationic amphiphiles: Equilibrium studies, *Biophys. J. 86*, 2392−2402.
52. Geourjon, C., and Deleage, G. (1995) SOPMA: Significant improvements in protein secondary structure prediction by consensus prediction from multiple alignments, *Comput. Appl. Biosci. 11*, 681−684.
53. Garnier, J., Gibrat, J. F., and Robson, B. (1996) GOR method for predicting protein secondary structure from amino acid sequence, *Methods Enzymol. 266*, 540−553.
54. Eftink, M. R. (1991) Fluorescence techniques for studying protein structure, *Methods Biochem. Anal. 35*, 127−205.
55. Fontana, A., Polverino de Laureto, P., de Filippis, V., Scaramella, E., and Zambonin, M. (1997) Probing the partly folded states of proteins by limited proteolysis, *Folding Des. 2*, R17−R26.
56. Kelly, S. M., and Price, N. C. (2000) The use of circular dichroism in the investigation of protein structure and function, *Curr. Protein Pept. Sci. 1*, 349−384.
57. Vucetic, S., Brown, C. J., Dunker, A. K., and Obradovic, Z. (2003) Flavors of protein disorder, *Proteins 52*, 573−584.
58. John, M., Briand, J. P., and Schnarr, M. (1996) A c-Jun activation domain peptide and its corresponding phosphopeptide have potential to adopt α-helical conformation, *Pept. Res. 9*, 71−78.
59. Tell, G., Perrone, L., Fabbro, D., Pellizzari, L., Pucillo, C., de Felice, M., Acquaviva, R., Formisano, S., and Damante, G. (1998) Structural and functional properties of the N transcriptional

activation domain of thyroid transcription factor-1: Similarities with the acidic activation domains, *Biochem. J. 329* (part 2), 395−403.
60. Baskakov, I. V., Kumar, R., Srinivasan, G., Ji, Y. S., Bolen, D. W., and Thompson, E. B. (1999) Trimethylamine *N*-oxide-induced cooperative folding of an intrinsically unfolded transcription-activating fragment of human glucocorticoid receptor, *J. Biol. Chem. 274*, 10693−10696.
61. Hershey, P. E., McWhirter, S. M., Gross, J. D., Wagner, G., Alber, T., and Sachs, A. B. (1999) The Cap-binding protein eIF4E promotes folding of a functional domain of yeast translation initiation factor eIF4G1, *J. Biol. Chem. 274*, 21297−21304.
62. Campbell, K. M., Terrell, A. R., Laybourn, P. J., and Lumb, K. J. (2000) Intrinsic structural disorder of the C-terminal activation domain from the bZIP transcription factor Fos, *Biochemistry 39*, 2708−2713.
63. Dawson, R., Muller, L., Dehner, A., Klein, C., Kessler, H., and Buchner, J. (2003) The N-terminal domain of p53 is natively unfolded, *J. Mol. Biol. 332*, 1131−1141.
64. Sanchez-Puig, N., Veprintsev, D. B., and Fersht, A. R. (2005) Human full-length securin is a natively unfolded protein, *Protein Sci. 14*, 1410−1418.
65. Sanchez-Puig, N., Veprintsev, D. B., and Fersht, A. R. (2005) Binding of natively unfolded HIF-1α ODD domain to p53, *Mol. Cell 17*, 11−21.
66. Yang, X. J. (2005) Multisite protein modification and intramolecular signaling, *Oncogene 24*, 1653−1662.
67. Morimoto, R. I. (2002) Dynamic remodeling of transcription complexes by molecular chaperones, *Cell 110*, 281−284.
68. Bentley, D. L. (1995) Regulation of transcriptional elongation by RNA polymerase II, *Curr. Opin. Genet. Dev. 5*, 210−216.
69. Roeder, R. G. (1996) The role of general initiation factors in transcription by RNA polymerase II, *Trends Biochem. Sci. 21*, 327−335.
70. Smith, C. L., and Peterson, C. L. (2005) ATP-dependent chromatin remodeling, *Curr. Top. Dev. Biol. 65*, 115−148.
71. Myers, L. C., and Kornberg, R. D. (2000) Mediator of transcriptional regulation, *Annu. Rev. Biochem. 69*, 729−749.
72. Dyson, H. J., and Wright, P. E. (2005) Intrinsically unstructured proteins and their functions, *Nat. Rev. Mol. Cell. Biol. 6*, 197−208.
73. Dunker, A. K., Lawson, J. D., Brown, C. J., Williams, R. M., Romero, P., Oh, J. S., Oldfield, C. J., Campen, A. M., Ratliff, C. M., Hipps, K. W., Ausio, J., Nissen, M. S., Reeves, R., Kang, C., Kissinger, C. R., Bailey, R. W., Griswold, M. D., Chiu, W., Garner, E. C., and Obradovic, Z. (2001) Intrinsically disordered protein, *J. Mol. Graphics Modell. 19*, 26−59.
74. Kyte, J., and Doolittle, R. F. (1982) A simple method for displaying the hydropathic character of a protein, *J. Mol. Biol. 157*, 105−132.
75. Gasteiger, E. H. C., Gattiker, A., Duvaud, S., Wilkins, M. R., Appel, R. D., Bairoch, A. (2005) Protein identification and analysis tools on the ExPASy server, in *The Proteomics Protocols Handbook* (Walker, J. M., Ed.) pp 571−607, Humana Press, Totowa, NJ.
76. Iakoucheva, L. M., Radivojac, P., Brown, C. J., O'Connor, T. R., Sikes, J. G., Obradovic, Z., and Dunker, A. K. (2004) The importance of intrinsic disorder for protein phosphorylation, *Nucleic Acids Res. 32*, 1037−1049.
77. MacArthur, M. W., and Thornton, J. M. (1991) Influence of proline residues on protein conformation, *J. Mol. Biol. 218*, 397−412.
78. Doolittle, R. F. (1989) Redundancies in protein sequences, in *Predictions of Protein Structure and the Principles of Protein Conformation*, pp 599−623, Plenum Press, New York.
79. Cox, M. M., and Nelson, D. L. (2000) *Lehninger Principles of Biochemistry*, 3rd ed., W. H. Freeman, New York.
80. Zhong, M., Kim, S. J., and Wu, C. (1999) Sensitivity of *Drosophila* heat shock transcription factor to low pH, *J. Biol. Chem. 274*, 3135−3140.
81. Kato, T., Hamada, D., Fukui, T., Hayashi, M., Honda, T., Murooka, Y., and Yanagihara, I. (2005) A pH-dependent conformational change in EspA, a component of the *Escherichia coli* O157:H7 type III secretion system, *FEBS J. 272*, 2773−2783.
82. Celinski, S. A., and Scholtz, J. M. (2002) Osmolyte effects on helix formation in peptides and the stability of coiled-coils, *Protein Sci. 11*, 2048−2051.
83. Naseem, F., and Khan, R. H. (2005) Characterization of a common intermediate of pea lectin in the folding pathway induced by TFE and HFIP, *Biochim. Biophys. Acta 1723*, 192−200.
84. Buck, M. (1998) Trifluoroethanol and colleagues: Cosolvents come of age. Recent studies with peptides and proteins, *Q. Rev. Biophys. 31*, 297−355.
85. Van Hoy, M., Leuther, K. K., Kodadek, T., and Johnston, S. A. (1993) The acidic activation domains of the GCN4 and GAL4 proteins are not α helical but form β sheets, *Cell 72*, 587−594.
86. Wang, A., and Bolen, D. W. (1997) A naturally occurring protective system in urea-rich cells: Mechanism of osmolyte protection of proteins against urea denaturation, *Biochemistry 36*, 9101−9108.
87. Tompa, P., Szasz, C., and Buday, L. (2005) Structural disorder throws new light on moonlighting, *Trends Biochem. Sci. 30*, 484−489.
88. Bharadwaj, S., Ali, A., and Ovsenek, N. (1999) Multiple components of the HSP90 chaperone complex function in regulation of heat shock factor 1 in vivo, *Mol. Cell. Biol. 19*, 8033−8041.
89. Baler, R., Zou, J., and Voellmy, R. (1996) Evidence for a role of Hsp70 in the regulation of the heat shock response in mammalian cells, *Cell Stress Chaperones 1*, 33−39.
90. Kumar, R., Volk, D. E., Li, J., Lee, J. C., Gorenstein, D. G., and Thompson, E. B. (2004) TATA box binding protein induces structure in the recombinant glucocorticoid receptor AF1 domain, *Proc. Natl. Acad. Sci. U.S.A. 101*, 16425−16430.
91. Warnmark, A., Wikstrom, A., Wright, A. P., Gustafsson, J. A., and Hard, T. (2001) The N-terminal regions of estrogen receptor α and β are unstructured in vitro and show different TBP binding properties, *J. Biol. Chem. 276*, 45939−45944.
92. Mason, P. B., and Lis, J. T. (1997) Cooperative and competitive protein interactions at the Hsp70 promoter, *J. Biol. Chem. 272*, 33227−33233.

BI061124C